Stainless steel is a promising electrode material for anodes of microbial fuel cells

Diana Pocaznoi, Amandine Calmet, Luc Etcheverry, Benjamin Erable and Alain Bergel*

The abilities of carbon cloth, graphite plate and stainless steel to form microbial anodes were compared under identical conditions. Each electrode was polarised at −0.2 V *vs.* SCE in soil leachate and fed by successive additions of 20 mM acetate. Under these conditions, the maximum current densities provided were on average 33.7 A m^{-2} for carbon cloth, 20.6 A m^{-2} for stainless steel, and 9.5 A m^{-2} for flat graphite. The high current density obtained with carbon cloth was obviously influenced by the three-dimensional electrode structure. Nevertheless, a fair comparison between flat electrodes demonstrated the great interest of stainless steel. The comparison was even more in favour of stainless steel at higher potential values. At +0.1 V *vs.* SCE stainless steel provided up to 35 A m^{-2}, while graphite did not exceed 11 A m^{-2}. This was the first demonstration that stainless steel offers a very promising ability to form microbial anodes. The surface topography of the stainless steel did not significantly affect the current provided. Analysis of the voltammetry curves allowed two groups of electrode materials to be distinguished by their kinetics. The division into two well-defined kinetics groups proved to be appropriate for a wide range of microbial anodes described in the literature.

Introduction

Stainless steels are common industrial materials that have high mechanical properties and long-term resistance to corrosion and are commercially available in many different compositions and morphologies. Microbial fuel cells (MFCs) and their related applications are emerging technologies based on the catalysis of electron transfer by microbial biofilms that develop on the electrode surfaces.[1,2] The nature, morphology and physicochemical properties of the electrodes are obviously of major importance in the design of microbially catalysed anodes and cathodes. As can be seen in recent reviews devoted to electrode materials for MFCs, the vast majority of studies have used carbon and graphite electrodes.[3–6] Many different morphologies (plates, papers, cloths, brushes, felts, nanotubes, …) and various chemical and physical surface treatments have been investigated for carbon and graphite electrodes. In contrast, stainless steels remain poorly investigated in the MFC domain in spite of their interesting advantages. Stainless steel offers a large range of engineering possibilities for scaling up electrodes. It allows solid, cost-effective, easy-to-handle equipment to be built, which is stable in the long-term and easy to maintain.

Stainless steels have already proved to be efficient in designs for microbial cathodes used in MFCs and related technologies. Immersed in aerated marine seawater, stainless steel cathodes allowed the development of microbial biofilms that exhibited high catalytic properties for oxygen reduction[7] and have been implemented in fuel cells.[8] In the field of microbial electrosynthesis, stainless steel cathodes colonised by *Geobacter sulfurreducens* cells have reduced fumarate to succinate at current densities up to 20.5 A m^{-2}.[9] In this case, using stainless steel multiplied the current density by a factor of 27 with respect to the values obtained with graphite under similar conditions. To the best of our knowledge, the current density obtained with stainless

Laboratoire de Génie Chimique, CNRS-Université de Toulouse (INPT), 4 allée Emile Monso BP 84234, 31432 Toulouse, France. E-mail: alain.bergel@ensiacet.fr; Tel: +33 5 34 32 36 73

Broader context

Early in the 21st century, it was discovered that microbial cells that spontaneously adhered to the surfaces of electrodes could become very efficient electro-catalysts. This new concept has been used in many promising applications like microbial fuel cells, microbial electrolysis and microbial electrosynthesis. Among more than three thousands articles devoted to these emerging technologies, less than a tenth has chosen stainless steel as the anode material, while the vast majority has used graphite and carbon. Here, it is demonstrated that stainless steel can develop microbial anodes producing higher current densities than graphite.

steel colonised by *Geobacter sulfurreducens* cells was the highest value reported so far for microbial cathodes. Obviously, these high current densities obtained under polarisation at low potential (−0.6 V *vs.* SCE) would not be relevant to MFC cathodes but can be exploited in electrosynthesis.

A few attempts have also pointed out some interesting properties of stainless steels for the design of microbial anodes.[10,11] Dumas *et al.* used a stainless steel anode in a marine MFC but the power provided remained low.[12] The studies performed under polarisation in three-electrode set-ups have given the most promising data. With a pure culture of *Geobacter sulfurreducens* Dumas *et al.*[13] obtained 2.4 A m^{-2} at +0.2 V *vs.* Ag/AgCl for the oxidation of acetate. With a natural biofilm formed from marine sediment, a current density of 3.1 A m^{-2} was obtained at +0.1 V *vs.* SCE.[14] The current density was then increased to 4 A m^{-2} by using a natural biofilm scraped from harbour equipment as inoculum.[15] The current density finally rose to 8.2 A m^{-2} with respect to the projected surface area of the electrode at −0.1 V *vs.* SCE by replacing the stainless steel plate by a stainless steel grid.[15] This value can be compared to the current densities obtained with carbon or graphite electrodes. To our knowledge, the highest current density reported in the literature for a carbon or a graphite microbial anode is 30.8 A m^{-2}.[16,17] This value was obtained with a three-dimensional carbon fibre electrode[17] with a biofilm formed from a wastewater-derived biofilm and resulted from clever optimisation of the porosity of the electrode. The anode was fed with acetate and provided this current density under polarisation at +0.2 V *vs.* Ag/AgCl (+0.155 V *vs.* SCE). Considering that the very few attempts made with stainless steel anodes produced current densities around 25% of the highest values reported so far with carbon and graphite suggests that stainless steel is worthy of interest and deserves to be investigated much further with a view to designing microbial anodes.

The objective of this work was to compare the ability of carbon and stainless steel materials under identical conditions to form microbial anodes. The 254SMO stainless steel grade was chosen because of its remarkable resistance to corrosion. It is recommended for use in the harshest chemical conditions, such as hydrofluoric, sulphuric or phosphoric acid environments, even at elevated temperatures. It is especially suited for high-chloride environments such as seawater. The pitting potential in seawater is of the order of 1000 mV/SCE, a value considerably higher than the open circuit potential of any cathode used in MFCs. In a fuel cell, the potential of the anode never exceeds the open circuit potential of the cathode. 254SMO stainless steel MFC anodes are consequently not at any risk of pitting corrosion, even in benthic environments. This grade is also resistant to embrittlement by hydrogen sulphide up to partial pressures of 1 bar and temperatures of 60 °C. Moreover, it is not affected by galvanic corrosion in contact with titanium; this is why titanium wires were used to connect the anode to the electrical circuit.

To make the comparison rigorous, experiments were performed under well-controlled electrochemical conditions using a 3-electrode electrochemical set-up. Leachate extracted from a soil was used as the inoculum because we have some experience with this inoculum source. The anodes were formed under constant polarisation at −0.2 V *vs.* SCE with successive additions of 20 mM acetate. This procedure allowed current densities in the range 32 to 36 A m^{-2} to be reproducibly obtained here with carbon cloth electrodes. These are the highest current densities reported so far. Actually, microbial anodes have provided up to 66 A m^{-2} on platinum electrodes,[18] but only in a very particular case that exploited the properties of ultra-microelectrodes.[19] The performance of the different materials was thus compared here under the best possible conditions with respect to the state of the art. Graphite plates were used to determine the performance of flat electrodes, without the enhancing effect of the 3-D structure that was beneficial in carbon cloth electrodes. The currents obtained with a flat graphite sheet could thus be directly compared to those provided by smooth stainless steel. Stainless steel electrodes with surface micro- and macro-structuring were also investigated with the objective of increasing the interaction between the biofilm and the material surface. Finally, cyclic voltammetry curves were recorded at a low scan rate in order to compare the different materials over a wide range of potential values.

Results and discussion

Chronoamperometry with different electrode materials

Four electrochemical reactors were run in parallel with the same inoculum but different electrode materials in each: carbon cloth, and smooth, macro-structured or micro-structured stainless steel (run #1). The reactors were initially fed with 20 mM acetate and the electrodes were polarized at −0.2 V *vs.* SCE. The current showed similar evolution for each electrode (Fig. 1, run #1). The initial lag-time was very short; the oxidation current began to increase after only 12 hours. After around two days of polarisation, the current showed a maximum and started to drop because of acetate depletion. Adding acetate to a concentration of 20 mM made the current increase again. For each electrode, the maximum current densities were generally of the same order of magnitude for the second, third and fourth acetate additions.

A similar experimental run achieved with a fresh inoculum and another four parallel reactors (run #2) led to identical current variations and current densities. A total of 11 independent experiments were performed using five fresh inoculum samples. The experiments were organised in such a way as to test each

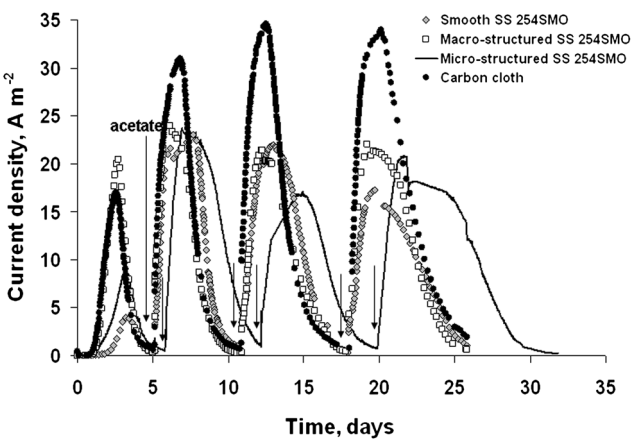

Fig. 1 Chronoamperometry curves recorded on carbon cloth, smooth stainless steel, macro-structured stainless steel, and micro-structured stainless steel under constant polarisation at −0.2 V *vs.* SCE (run #1).

anode material with at least two different inoculum samples (Table 1). The currents were thus shown not to be significantly affected by the difference in inoculum samples. For each experiment the third and fourth acetate additions led to similar currents, which indicated fair biofilm stabilization. The average current densities given in Table 1 were calculated with the third and fourth current peaks of each experiment, meaning that the discussion was based on 22 measurements coming from 11 independent experiments.

The 3 independent experiments performed with the carbon cloth anodes gave maximum current densities of 33.7 A m^{-2} (average of 6 measurements in the range 32 to 36 A m^{-2}). These current densities were the highest values reported so far in the literature with microbial anodes. The high performance obtained here resulted from our previous work to determine optimal conditions for biofilm formation from soil inocula (leachate preparation, polarisation potential, acetate concentration, KCl addition, *etc.*).[20,21] Moreover, the previous work was carried out at ambient temperature, while the present experiments were performed at 40 °C, which had been determined as the optimal temperature for the inoculum source used here.[22] Finally, the three-dimensional structure of the cloth electrode had also an essential positive effect as demonstrated by Schroeder's group. They have obtained current densities of the same order of magnitude (30.8 A m^{-2} at +0.2 V *vs.* Ag/AgCl) with three-dimensional electrodes composed of carbon fibres with well-defined diameters ranging from 0.1 to 10 μm.[16,17] The authors have observed that the current density increased when the fibre diameter decreased until it reached approximately 1 μm. They attributed the high current density obtained to the high electrode porosity of over 99%, as well as to the fibre diameter itself, which ensured the formation of thick and continuous biofilms. In the present work, the cloth electrodes were made of 8 μm diameter fibres that were assembled into around 200 μm diameter wires woven to make the final cloth (Fig. 2A). The global morphology and the fibre diameter were not the same as those of the previously reported studies but the final result in terms of biofilm structure can be considered to be similar: the biofilm formed here appeared to penetrate the structure of the electrode deeply and exploit its three-dimensional configuration optimally to develop a large surface area (Fig. 2A).

Always considering the last two acetate additions, no significant difference was observed between smooth, macro- and micro-structured stainless steel electrodes. The current density provided by stainless steel electrodes was 20.6 A m^{-2} (average of 12 measurements ranging from 17 to 25 A m^{-2}). The flat graphite electrodes gave 9.5 A m^{-2} (average of 4 measurements ranging from 7.5 to 11 A m^{-2}). The comparison of flat graphite and stainless steel showed an obvious advantage of stainless steel. Actually, the current densities reported in the literature with carbon and graphite electrodes were often higher than those reported with stainless steel because of the enhancement effect of the three-dimensional structure that benefited the carbon or graphite. In contrast, the present comparison of flat electrodes under identical conditions stressed the great interest of stainless steel, which gave current densities twice as high as those obtained with graphite.

The current densities obtained here were five times higher than the values reported with flat stainless steel anodes so far[14,15] and even higher than current densities obtained with stainless steel grid anodes.[15] The experience we have gained in exploiting the soil inoculum optimally may be a part of the explanation.[21] Another cause can be found in the control of the oxide layer that covers the surface of stainless steels. Stainless steel anodes implemented in a marine MFC have been shown to loose a part of their electroactivity at high potential values. The electroactivity decrease has been attributed to the modification of the oxide layer, which took on n-type semi-conductive properties at high potentials.[23] N-type semi-conduction of the surface layer obviously hampers anodic electron transfer. Actually, in the framework of corrosion research, it has been demonstrated that stainless steel oxide layers can have n-type semi-conductive properties at potentials higher than their flat-band value.[24] The flat-band value depends significantly on the solution and the operating conditions.[25,26] It has generally been measured in marine aerobic media in corrosion studies. Recently, the flat-band value of superaustenitic stainless steel has been assessed around +0.12 V/SHE (−0.12 V/SCE) under anaerobic conditions in the *Geobacter sulfurreducens* growth medium.[27] The potential of −0.2 V/SCE, which was appropriate to exploit the soil inoculum on carbon anodes, seemed also low enough to avoid the formation of a detrimental n-type semi-conductive layer on the anode surface. This postulate, which fits the data reported in the literature perfectly, must now be validated by further material analysis.

Electrode topography

The roughness of stainless steel electrodes has been shown to have a significant effect on the formation of microbial cathodes from a pure culture of *Geobacter sulfurreducens*.[28] The purpose here was to evaluate whether a similar effect could be observed with wild natural biofilms. Flint *et al.* have postulated that microbial adhesion is favoured by entrapment of the cells on the surfaces that present an average roughness value (R_a) in the range of the

Table 1 Current densities obtained with electrodes of different materials

Electrode material	Number of measurements/number of different inoculum samples	Current density A m^{-2}	
		Average value	Minimum and maximum
Smooth stainless steel	4/2	19.7	17–23
Macro-structured stainless steel	4/2	20.5	18–22
Micro-structured stainless steel	4/2	21.5	17–25
Graphite	4/2	9.5	7.5–11
Carbon cloth	6/3	33.7	32–36

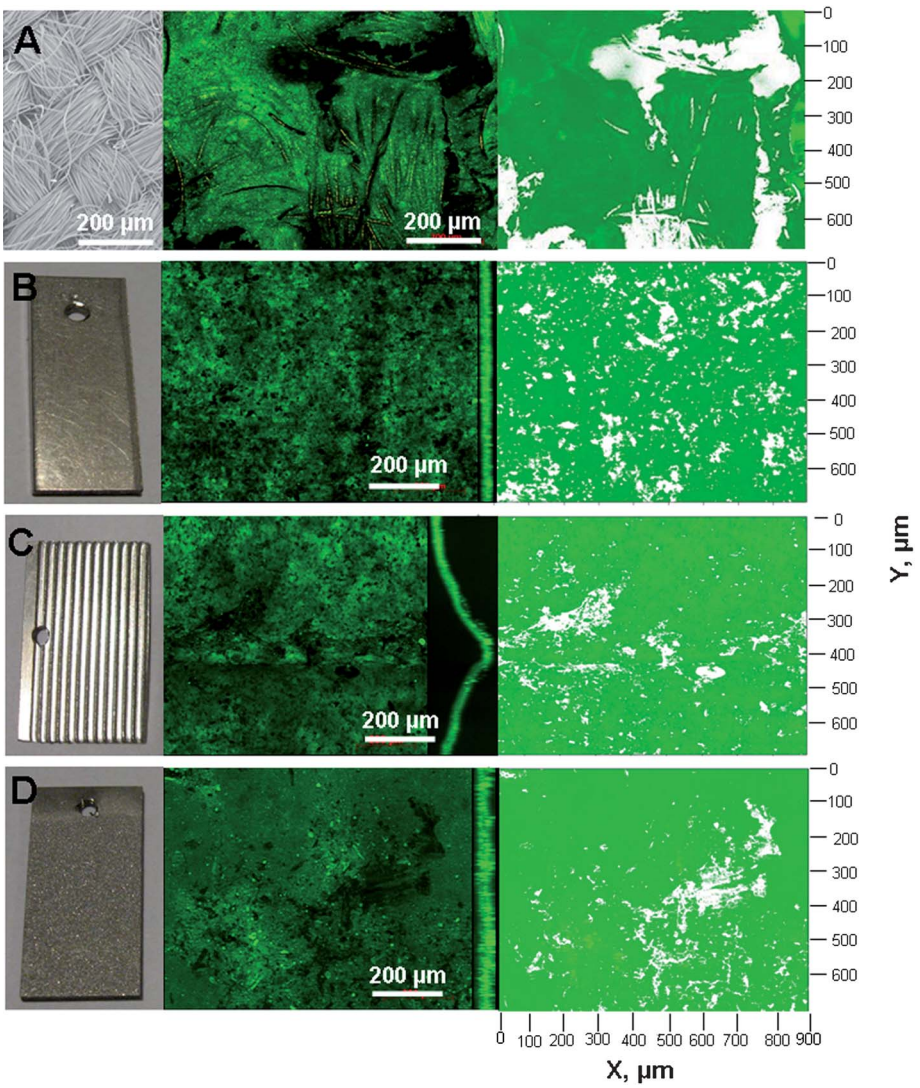

Fig. 2 Epifluorescence imaging of anodes developed under constant potential (run #2) on (A) carbon cloth, (B) smooth stainless steel, (C) macro-structured smooth stainless steel, and (D) micro-structured smooth stainless steel. From left to right: macroscopic view of the clean electrode, epifluorescence image and treated images to assess the surface coverage ratio by the biofilm.

size of microbial cells, *i.e.* around one to a few micrometres.[29] Working with *Pseudomonas* sp., *Listeria monocytogenes* and *Candida lipolytica* Hilbert *et al.* showed that roughness of less than 0.9 µm did not affect microbial adhesion on 316 stainless steel.[30] On the other hand, Scheuerman *et al.* observed that surface irregularities increased the quantity of *Pseudomonas aeruginosa* and *fluorescens* on silicone samples, but that a roughness greater than 10 µm had no additional effect.[31] This tends to confirm the general postulate of Flint *et al.*, although other studies have demonstrated more complex behaviours. Allion *et al.* studying *Staphylococcus aureus* on 304 stainless steel[32] noted that adhesion was reduced on surfaces with a R_a of 2.1–2.3 µm compared with surfaces with R_a of 1.4 µm. In this case the level of bacterial adhesion was decreased by a factor of ten on surfaces with the highest roughness value. Actually, the depth and width of the grooves were compatible with the size of the bacterial cells and allowed cell trapping, but also limited the number of adherent cells. The simple conclusion is that it is difficult to predict the effect of surface topography on bacterial adhesion and so on biofilm formation and electroactivity development. A roughness value $R_a = 5$ µm was chosen for micro-structuring because it was in the range where it could have a major effect on microbial adhesion according to Flint's postulate.

Macro-structuring was also tested. Macro-structuring was achieved with large lines with the intention of favouring microbial development at the bottom of the valleys. No significant difference of the currents provided was observed here between smooth, micro- and macro-structured stainless steel electrodes. This result was in contrast to the observations previously made with stainless steel cathodes formed from a pure culture of *Geobacter sulfurreducens*.[28] In the previous study, average surface roughness values $R_a = 2.0$ to 4.0 µm increased the current by a factor of 1.6 with respect to the smooth surface. The surface roughness affected the current density by encouraging different colonisation patterns on the electrode surface.[28] These observations were done with pure cultures in a synthetic medium, the

composition of which was minimal. Under such conditions, the microbial colonisation at the end of the experiments was very low. The electroactive biofilms were made up of small microbial colonies, or even groups of a few cells only, scattered on the electrode surface. The biofilm morphology was very different in the present work, as can be seen on the epifluorescence images recorded at the end of polarisation (Fig. 2B–D). Whatever was the surface structure of the electrode, the biofilms achieved a uniform, almost complete coverage with thickness around 50–60 μm. The biofilm grown on the micro-structured surface was slightly thicker (Fig. 2C) but this small difference did not affect the current densities provided. The rich environment that served as inoculum here, in terms of both microbial diversity and nutriment content, favoured the growth of well-developed biofilms that masked a possible effect of the surface structuring. As a general conclusion, it can be claimed that the possible effect of electrode topography depends strongly on the inoculum and medium composition, assuming that rich media that favour fast biofilm formation tend to mask a possible effect of the surface topography.

Electrochemical kinetics on different electrode materials

From time to time, the chronoamperometry experiments were interrupted to record cyclic voltammetry (CV) curves when the electrode provided current densities as close as possible to the maximum values. Fig. 3 presents CV recorded at 1, 10 and 100 mV s^{-1} and finally back to 1 mV s^{-1} on smooth stainless steel and carbon cloth electrodes (day 13 for stainless steel electrode and day 12 for carbon cloth electrode, run #2). The first and last CVs both recorded at 1 mV s^{-1} were strictly identical (the last CV was not plotted on the figure because it was perfectly superimposed on the first one), showing that the biofilm was not disturbed by the successive CV scans. Cyclic voltammetry has already been shown to be an efficient non-destructive technique for studying electroactive biofilms.[33,34]

The oxidation started from −0.50 V *vs.* SCE independently of the electrode material. CVs performed at 1 and 10 mV s^{-1} were identical and CV recorded at 100 mV s^{-1} diverged slightly from the others at the highest potential values. Thus, the electrodes gave a steady state response up to 10 mV s^{-1} and were not far from steady state even at 100 mV s^{-1}. Such stability of the cyclic voltammetry at high scan rates indicated a remarkable ability of the anodes to achieve fast electron transfer. It was also checked that the current densities measured at −0.2 V *vs.* SCE on the CV curves were equal to the values recorded during chronoamperometry just before the interruption. This confirmed that CV gave the steady state electrode kinetics.

Fig. 4A illustrates cyclic voltammograms at low scan rate (1 mV s^{-1}) recorded on carbon cloth, smooth stainless steel, micro- and macro-structured stainless steel electrode (run #2) and graphite (run #3). A marked difference appeared in the electrochemical kinetics between the stainless steel electrodes on the one hand, and carbon cloth and graphite electrodes on the other hand. The carbon and graphite electrodes reached a maximum current density plateau (J_{max}) from −0.25 V *vs.* SCE, while stainless steel electrodes reached their J_{max} value only above +0.1 V *vs.* SCE. In terms of electrochemical kinetics, carbon and graphite exhibited better performance, because they were able to provide their J_{max} at lower potentials. Nevertheless, it must be borne in mind that carbon cloth benefited from a favourable 3-D morphology. A fair comparison between flat-surface electrodes showed that stainless steel gave a higher current density than graphite at any potential (Fig. 4A). The interest of stainless steel was even more obvious at higher potential values. CVs recorded during different runs showed that stainless steel electrodes can provide up to 35 or 38 A m^{-2} at +0.1 and +0.3 V *vs.* SCE, respectively, while flat graphite never exceeded 11 A m^{-2}. It may be noted that at the highest potential values the micro-structured electrodes sometimes provided higher current densities than the other stainless steel electrodes. Nevertheless, the difference in most voltammetry curves was not significant enough to reasonably conclude that micro-structuring may have a beneficial effect.

Fig. 4B represents the same curves as Fig. 4A but indicates the non-dimensional current I/I_{max} on the Y-axis. This standardised representation allowed two groups with different kinetic behaviour to be clearly distinguished. The first group, composed of the carbon cloth and graphite electrodes, exhibited a Nernst-type kinetics, which can be modelled by the conventional equation:[19]

$$I/I_{max} = 1/(1 + \exp[-F/RT\,(E - E_{1/2})])$$

where I/I_{max} is the non-dimensional current plotted on the Y-axis, E the potential (V *vs.* SCE) plotted on X-axis, F the Faraday constant (96 485 Coulomb per mol e^-), R the gas constant (8.3145 J mol^{-1} K^{-1}), T the temperature (313 K), and $E_{1/2}$ the anode potential at which $I/I_{max} = 1/2$. The theoretical curve plotted in Fig. 4B was calculated with the average $E_{1/2}$ value = −0.375 V/SCE that was extracted from the two experimental curves. The theoretical curve satisfactorily fitted the two experimental curves. The Nernstian shape of the experimental

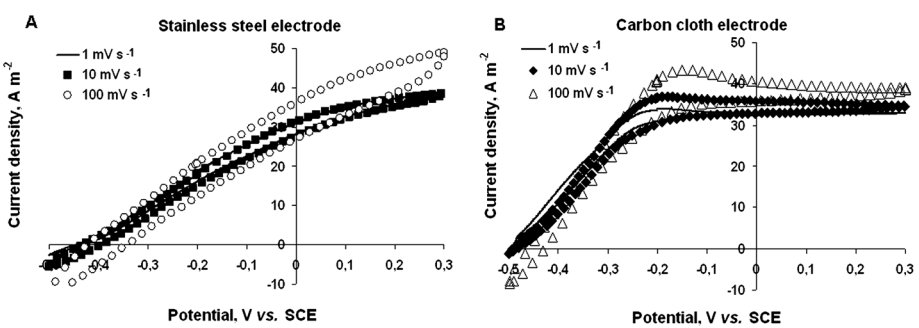

Fig. 3 Successive cyclic voltammetry curves recorded at different scan rates on (A) smooth stainless steel and (B) carbon cloth electrodes (run #2).

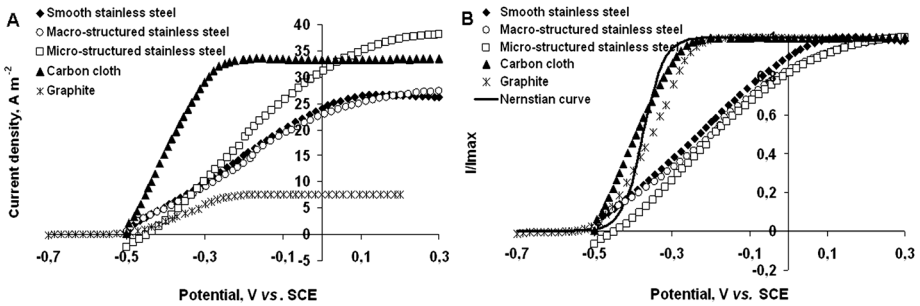

Fig. 4 Cyclic voltammetry curves recorded at 1 mV s^{-1} on electrodes of different materials (run #2). (A) Current density as a function of potential, (B) non-dimensional I/I_{max} as a function of potential and comparison with a theoretical Nernstian curve.

curves showed that the electron transfer between the electrode and the last redox compound in contact with the electrode surface was reversible and fast enough to ensure the Nernst equilibrium between the oxidized and reduced forms of the redox compound at all times. The interfacial electron transfer kinetics was so fast that activation effects could not be seen. The voltammetry curves kept the same shape at a scan rate of 10 mV s^{-1} and were hardly affected at 100 mV s^{-1}. This means that the interfacial electron transfer was fast enough to ensure the Nernst equilibrium at high scan rates. It can be concluded that carbon and graphite that were used here were excellent electrode materials for microbial anodes from the point of view of electrochemical kinetics.

The second set of I/I_{max}–E curves grouped together all the stainless steel electrodes, whatever their surface structuring. This group showed a less efficient interfacial electron transfer that required significant overpotential. The microbial anodes formed on stainless steel gave a higher current than those formed on flat graphite but stainless steel was revealed to be not able to ensure electron transfer that was as fast as that of graphite or carbon cloth. A significant improvement could consequently be made by further detailed kinetics studies that would manage to accelerate the electron transfer between stainless steel and anode respiring bacteria. This would be a very relevant research topic for the future.

Distinguishing between these two kinetics groups proved to have a broad applicability over the present work. CV curves recorded at a low scan rate (1 mV s^{-1}) on different electrode materials: carbon fibre electrode,[17] platinum,[18] glassy carbon,[33] modified graphite,[35] tin indium oxide[36] and polycrystalline graphite[37] were extracted from the literature and are plotted in Fig. 5 in the I/I_{max} non-dimensional form. The characteristics of each anode are reported in Table 2. The eight curves fitted into the two kinetics groups perfectly. Platinum, tin indium oxide and glassy carbon ensured Nernstian electron transfer, while carbon fibres and polycrystalline graphite coming from the literature were close to the curves obtained with stainless steel in the present work. The two types of kinetic behaviour are consequently not straightforwardly linked to the nature of the electrode. A general classification with graphite and carbon in one group and stainless steel in the other would not be relevant, as carbon and graphite electrodes could offer Nernstian kinetics or not. More surprisingly, the different anodes that did not lead to a Nernstian kinetics all had a pretty similar shape with a quite narrow range of I–E slopes.

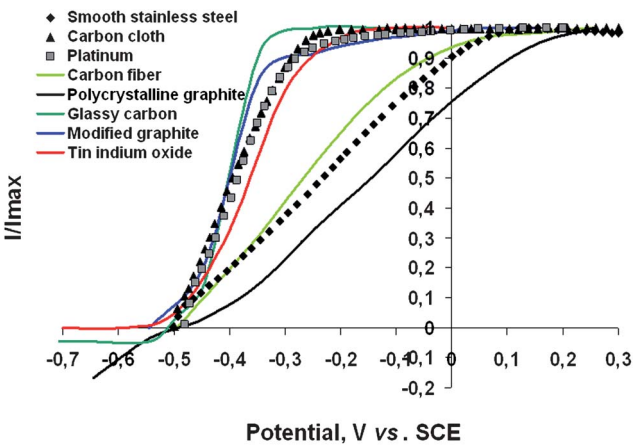

Fig. 5 Non-dimensional I/I_{max} ratio as a function of potential on electrodes of different materials from this work and the literature. The characteristics of each anode are reported in Table 2.

Experimental

Inoculum and medium preparation

Garden compost for organic cultivation (Eco-Terre) was used as an inoculum source. 1 L of garden compost was mixed with 1.5 L of distilled water containing 60 mM of potassium chloride and left for 24 hours with stirring. Then the mixture was centrifuged, and 20 mM of acetate was added into the leachate, which was used as the medium in the electrochemical reactors. The initial pH was around 7.5 and the initial conductivity was 12 mS cm^{-1}. The pH increased to 8.5–9 during the experiments. This alkalinisation was not linked to the electrochemical reactions but was due to the spontaneous evolution of the non-buffered compost leachate as already shown.[21] All the experiments were performed at 40 °C.

Electrodes

Stainless steel electrodes were of superaustenitic grade (254SMO, Outokumpu, UNS31254, composition Cr 19.9%; Ni 17.8%; Mo 6.0%; N 0.2%; C 0.01%; Fe complement). The 2.5 cm^2 electrodes were electrically connected with a 2 mm diameter screwed titanium wire. The micro-structured surfaces with R_a = 5 μm were obtained by sandblasting. The macro-structured surface was designed mechanically by scoring

Table 2 Experimental characteristics of the voltammetry curves plotted in Fig. 5

Electrode material	Inoculum	Scan rate, mV s^{-1}	Graphics/curve colour corresponding to Fig. 5	Reference
Smooth stainless steel	Soil leachate	1	◆	This work
Carbon cloth	Soil leachate	1	▲	This work
Platinum	Soil leachate	1	▢	18
Carbon fiber	Wastewater	1	Lime	17
Polycrystalline graphite	Wastewater	1	Black	37
Glassy carbon	*Geobacter Sulfurreducens*	1	Green	33
Modified graphite	*Geobacter Sulfurreducens*	5	Blue	35
Tin indium oxide	*Geobacter Sulfurreducens*	1	Red	36

micro-lines along the electrode (width 300 μm, depth 500 μm, angle 45°). Before the experiments, the stainless steel electrodes were cleaned with a 50–50% ethanol–acetone solution for 20 min under stirring to dissolve organic adsorbed species, then 20 min with a 2–20% fluorhydric–nitric acid solution to remove the oxide layer and were finally thoroughly rinsed in distilled water. The stainless steel electrodes could be stored with no particular precautions for days or weeks before use. Actually, the oxide layer reformed on the electrode surface when it was in contact with oxygen but it was reduced during the first hours of chronoamperometry. The role of the cleaning procedure was only to avoid the occurrence of reductive currents at the beginning of chronoamperometry, which would depend on the initial composition of the oxide layer. Nevertheless, from our previous experience, the initial presence or absence of old oxide layers did not affect the biofilm electroactivity because the value of the applied potential controlled the composition of the oxide layer after a few hours of polarisation.

Carbon cloth was provided by the PaxiTech society (Grenoble, France). New electrodes were used for each experiment after rinsing with distilled water. The 2 cm^2 electrodes were connected to the electrical circuit by a 1 mm diameter platinum wire (Heraeus). Graphite electrodes (Carbone Lorraine) were disks of 3 mm in diameter inserted in an insulating resin. They were cleaned by polishing followed by a thorough rinse with distilled water.

Electrochemical set-up

Experiments were performed using three-electrode systems, each composed of the working electrode under study, a saturated calomel reference electrode (SCE, Radiometer Analytical, +0.241 V *vs.* SHE) and a 6 cm^2 platinum grid as an auxiliary electrode. The electrochemical reactors contained 150 mL (runs #2–5) or 550 mL (run #1) of soil leachate. The electrodes were polarised using a VMP potentiostat (Bio-logic SA) and the current was recorded every 1800 s. Chronoamperometry was sometimes interrupted to perform cyclic voltammetries at 1, 10 and 100 mV s^{-1}. Additions of 20 mM acetate were made when the current dropped to zero. All the current densities were calculated with respect to the electrode projected surface areas.

Epifluorescence microscopy

Microbial biofilms were imaged by epifluorescence microscopy. The biofilms were stained with acridine orange 0.01% (A6014 Sigma) for 10 minutes, then washed carefully with distilled water and dried at ambient temperature. The samples were imaged with a Carl Zeiss AxioImager M2 microscope equipped for epifluorescence with an HBO 50 W ac mercury light source and the Zeiss 09 filter (excitor HP450–490, reflector FT 10, barrier filter LP520). Images were acquired with a monochrome digital camera (Evolution VF) every 0.5 μm along the *Z*-axis and the set of images was processed with the Axiovision® software.

Conclusions

Microbial anodes formed under identical conditions proved to be able to produce a higher current density when formed on stainless steel than on flat graphite (20.6 A m^{-2} compared with 9.5 A m^{-2} on average, under polarisation at −0.2 V *vs.* SCE). The comparison was even more in favour of stainless steel at higher potential values. For instance, the microbial anodes formed on stainless steel were able to provide up to 35 A m^{-2} at +0.1 V *vs.* SCE, while anodes formed on flat graphite did not exceed 11 A m^{-2}. Stainless steel is consequently a very promising candidate for the design of efficient microbial anodes, which now deserves to be investigated much more thoroughly. For the future, an essential research direction would be to decipher the electron transfer mechanisms that control the non-Nernstian kinetic behaviour evidenced here for stainless steel and also some carbon fibre electrodes. Actually, the carbon fibre electrodes that have given the highest current density reported in the literature had the same kinetic behaviour as stainless steel. Could this be a common feature of the most efficient microbial anodes?

Acknowledgements

This research was part of the "Agri-Elec" project funded by the French National Research Agency (ANR-08-BioE-001). J. M. Lameille from CEA-Saclay (France) is gratefully acknowledged for providing us with stainless steel and micro-structured electrodes and A. Müller from Laboratoire de Génie Chimique (Toulouse, France) for engineering the macro-sized stainless steel surfaces.

Notes and references

1 B. E. Logan, B. Hamelers, R. A. Rozendal, U. Schrorder, J. Keller, S. Freguia, P. Aelterman, W. Verstraete and K. Rabaey, *Environ. Sci. Technol.*, 2006, **40**, 5181–5192.
2 D. Pant, A. Singh, G. Van Bogaert, S. I. Olsen, P. S. Nigam, L. Diels and K. Vanbroekhoven, *RSC Adv.*, 2012, **2**, 1248–1263.
3 M. H. Zhou, M. L. Chi, J. M. Luo, H. H. He and T. Jin, *J. Power Sources*, 2011, **196**, 4427–4435.

4 A. Rinaldi, B. Mecheri, V. Garavaglia, S. Licoccia, P. Di Nardo and E. Traversa, *Energy Environ. Sci.*, 2008, **1**, 417–429.
5 Y. Qiao, S.-J. Bao and C. M. Li, *Energy Environ. Sci.*, 2010, **3**, 544–553.
6 J. C. Wei, P. Liang and X. Huang, *Bioresour. Technol.*, 2011, **102**, 9335–9344.
7 S. Dulon, S. Parot, M. L. Delia and A. Bergel, *J. Appl. Electrochem.*, 2007, **37**, 173–179.
8 A. Bergel, D. Feron and A. Mollica, *Electrochem. Commun.*, 2005, **7**, 900–904.
9 C. Dumas, R. Basseguy and A. Bergel, *Electrochim. Acta*, 2008, **53**, 2494–2500.
10 S. Srikanth, T. Pavani, P. N. Sarma and S. V. Mohan, *Int. J. Hydrogen Energy*, 2011, **36**, 2271–2280.
11 J. L. Lamp, J. S. Guest, S. Naha, K. A. Radavich, N. G. Love, M. W. Ellis and I. K. Puri, *J. Power Sources*, 2011, **196**, 5829–5834.
12 C. Dumas, A. Mollica, D. Feron, R. Basseguy, L. Etcheverry and A. Bergel, *Electrochim. Acta*, 2007, **53**, 468–473.
13 C. Dumas, R. Basseguy and A. Bergel, *Electrochim. Acta*, 2008, **53**, 5235–5241.
14 B. Erable, M. A. Roncato, W. Achouak and A. Bergel, *Environ. Sci. Technol.*, 2009, **43**, 3194–3199.
15 B. Erable and A. Bergel, *Bioresour. Technol.*, 2009, **100**, 3302–3307.
16 G. He, Y. Gu, S. He, U. Schröder, S. Chen and H. Hou, *Bioresour. Technol.*, 2011, **102**, 10763–10766.
17 S. L. Chen, H. Q. Hou, F. Harnisch, S. A. Patil, A. A. Carmona-Martinez, S. Agarwal, Y. Y. Zhang, S. Sinha-Ray, A. L. Yarin, A. Greiner and U. Schroder, *Energy Environ. Sci.*, 2011, **4**, 1417–1421.
18 D. Pocaznoi, B. Erable, M.-L. Delia and A. Bergel, *Energy Environ. Sci.*, 2012, **5**, 5287–5296.
19 *Electrochemical Methods*, ed. A. J. Bard and L. R. Faulkner, John Wiley & Sons, New York, 2nd edn, 2001, vol. 1, pp. 168–176.
20 B. Cercado-Quezada, M.-L. Delia and A. Bergel, *Bioresour. Technol.*, 2012, **101**, 2748–2754.
21 D. Pocaznoi, B. Erable, L. Etcheverry, M.-L. Delia and A. Bergel, *Phys. Chem. Chem.Phys.*, DOI: 10.1039/c2cp42571h.
22 B. Cercado-Quezada, M.-L. Delia and A. Bergel, *J. Appl. Electrochem.*, 2010, **40**, 225–232.
23 C. Dumas, A. Mollica, D. Feron, R. Basseguy, L. Etcheverry and A. Bergel, *Bioresour. Technol.*, 2008, **99**, 8887–8894.
24 V. L'Hostis, C. Dagbert and D. Féron, *Electrochim. Acta*, 2003, **48**, 1451–1458.
25 C. Marconnet, Y. Wouters, F. Miserque, C. Dagbert, J. P. Petit, A. Galerie and D. Féron, *Electrochim. Acta*, 2008, **54**, 123.
26 M. Faimali, E. Chelossi, F. Garaventa, C. Corra, G. Greco and A. Mollica, *Electrochim. Acta*, 2008, **54**, 148.
27 L. Pons, M.-L. Delia and A. Bergel, *Electrochim. Acta*, 2011, **56**, 2682–2688.
28 L. Pons, M.-L. Delia and A. Bergel, *Bioresour. Technol.*, 2011, **102**, 2678–2683.
29 S. H. Flint, J. D. Brooks and P. J. Bremer, *J. Food Eng.*, 2000, **43**, 235–242.
30 L. R. Hilbert, D. Bagge-Ravn, J. Kold and L. Gram, *Int. Biodeterior. Biodegrad.*, 2003, **52**, 175–185.
31 T. R. Scheuerman, A. K. Camper and M. A. Hamilton, *J. Colloid Interface Sci.*, 1998, **208**, 23–33.
32 A. Allion, J. P. Baron and L. Boulange-Petermann, *Biofouling*, 2006, **22**, 269–278.
33 E. Marsili, J. B. Rollefson, D. B. Baron, R. M. Hozalski and D. R. Bond, *Appl. Environ. Microbiol.*, 2008, **74**, 7329–7337.
34 Y. Yuan, S. Zhou, N. Xu and L. Zhuang, *Colloids Surf., B*, 2011, **82**, 641–646.
35 K. Fricke, F. Harnisch and U. Schroder, *Energy Environ. Sci.*, 2008, **1**, 144–147.
36 A. Jaina, G. Gazzolaa, A. Panzerab, M. Zanonic and E. Marsili, *Electrochim. Acta*, 2011, **56**, 10776–10785.
37 F. Harnisch, C. Koch, S. A. Patil, T. Huebschmann, S. Mueller and U. Schroeder, *Energy Environ. Sci.*, 2011, **4**, 1265–1267.